

RESEARCH PAPER

Effects of systemic inhibitors of acid-sensing ion channels 1 (ASIC1) against acute and chronic mechanical allodynia in a rodent model of migraine

Correspondence Eric Lingueglia and Anne Baron, Université Côte d'Azur, CNRS, Institut de Pharmacologie Moléculaire et Cellulaire, Valbonne, France. E-mail: lingueglia@ipmc.cnrs.fr; anne.baron@ipmc.cnrs.fr

Received 7 March 2018; **Revised** 28 June 2018; **Accepted** 26 July 2018

Clément Verkest^{1,2,3}, Emilie Piquet^{3,4}, Sylvie Diochot^{1,2,3}, Mélodie Dauvois¹, Michel Lanteri-Minet^{3,4,5}, Eric Lingueglia^{1,2,3,*}  and Anne Baron^{1,2,3,*} 

¹Université Côte d'Azur, CNRS, Institut de Pharmacologie Moléculaire et Cellulaire, Valbonne, France, ²LabEx Ion Channel Science and Therapeutics, Valbonne, France, ³FHU InovPain, Université Côte d'Azur, Nice, France, ⁴CHU Nice, Hôpital Cimiez, Département d'évaluation et de traitement de la douleur, Nice, France, and ⁵Inserm/UdA, U1107, Neuro-Dol, Trigeminal Pain and Migraine, Université d'Auvergne, Clermont-Ferrand, France

*E. L. and A. B. contributed equally to this work.

BACKGROUND AND PURPOSE

Acid-sensing ion channels (ASICs) are neuronal proton sensors emerging as potential therapeutic targets in pain of the orofacial region. Amiloride, a non-specific ASIC blocker, has been shown to exert beneficial effects in animal models of migraine and in patients. We explored the involvement of the ASIC1-subtype in cutaneous allodynia, a hallmark of migraine affecting cephalic and extra-cephalic regions in about 70% of migrainers.

EXPERIMENTAL APPROACH

We investigated the effects of systemic injections of amiloride and mambalgin-1, a specific inhibitor of ASIC1a- and ASIC1b-containing channels, on cephalic and extra-cephalic mechanical sensitivity in a rodent model of acute and chronic migraine induced by i.p. injections of isosorbide dinitrate.

KEY RESULTS

I.v. injections of these inhibitors reversed cephalic and extra-cephalic acute cutaneous mechanical allodynia in rats, a single injection inducing a delay in the subsequent establishment of chronic allodynia. Both mambalgin-1 and amiloride also reversed established chronic allodynia. The anti-allodynic effects of mambalgin-1 were not altered in ASIC1a-knockout mice, showing the ASIC1a subtype is not involved in these effects which were comparable to those of the anti-migraine drug sumatriptan and of the preventive drug topiramate on acute and chronic allodynia respectively. A single daily injection of mambalgin-1 also had a significant preventive effect on allodynia chronification.

CONCLUSIONS AND IMPLICATIONS

These pharmacological data support the involvement of peripheral ASIC1-containing channels in migraine cutaneous allodynia as well as in its chronification. They highlight the therapeutic potential of ASIC1 inhibitors as both an acute and prophylactic treatment for migraine.

Abbreviations

ASIC, acid-sensing ion channel; CSD, cortical spreading depression; i.pl., intraplantar; ISDN, isosorbide dinitrate; KO, knockout; Mamb-1, mambalgin-1; TG, trigeminal; TNC, trigeminal nucleus caudalis

Introduction

Migraine is a major contributor to public ill health (Vos *et al.*, 2016). Its pathogenetic mechanisms are still poorly understood (Goadsby *et al.*, 2017) and possibly include extracellular acidification. Cortical spreading depression (CSD), considered to be the neurophysiological correlate of migraine aura, could activate and sensitize trigeminal (TG) meningeal nociceptors (Karatas *et al.*, 2013) through local release of extracellular compounds (K^+ , **ATP**, **NO**), and dural sterile inflammation and ischaemia associated with extracellular acidification also involving mast cell degranulation (Rozniecki *et al.*, 1999; Levy, 2009). Subsequent sensitization of central pathways would cause the cephalic and extra-cephalic cutaneous allodynia (Edelmayer *et al.*, 2009; Burstein *et al.*, 2010; Boyer *et al.*, 2014) reported by 70% of migrainers during migraine attacks (Lipton *et al.*, 2008). Per year, approximately 2.5% of episodic migrainers become chronic migrainers, with at least 15 days of headache per month (Bigal *et al.*, 2008; Lipton *et al.*, 2015), showing acute cutaneous allodynia during attacks but also interictal allodynia between them (Nahman-Averbuch *et al.*, 2018). Cutaneous allodynia is now considered as a marker and a risk factor for chronic migraine (Louter *et al.*, 2013), chronic migraine onset being increased by 30% among episodic migrainers, and chronic migraine persistence being increased by 15% in chronic migrainers (Scher *et al.*, 2017).

Preclinical migraine models in rodents are based on human observations. NO donors such as **nitroglycerin** (NTG) (Ashina *et al.*, 2013) and nitrate-based drugs with slower pharmacokinetics like **isosorbide dinitrate** (ISDN) used in the treatment of cardiovascular disease (Iversen *et al.*, 1992; Olesen and Ashina, 2015; Hansen and Olesen, 2017) trigger a delayed-migraine attack associated with cutaneous facial and extra-facial allodynia (Thomsen *et al.*, 1996). In rodents, NO donors evoke elevated **CGRP** blood levels, meningeal inflammation, photo and phonophobia, sensitization of central neurons of the trigeminal nucleus caudalis (TNC), cephalic and extra-cephalic allodynia, as well as spontaneous facial pain. The effectiveness of clinically relevant treatments like **sumatriptan**, CGRP antagonists and antibodies, anti-inflammatory drugs, or prophylactic drugs like **propranolol** and **topiramate** further support the relevance of these animal models of migraine (Bates *et al.*, 2010; Jansen-Olesen *et al.*, 2013; Pradhan *et al.*, 2014; Farkas *et al.*, 2016; Goadsby *et al.*, 2017; Harris *et al.*, 2017; Schytz *et al.*, 2017). Effects of systemic ISDN injections were recently described in rats, with a facilitation of C-fibre-evoked responses in 50% of second-order central neurons (Flores Ramos *et al.*, 2017; Dallel *et al.*, 2018), leading to cutaneous pain sensitization.

Acid-sensing ion channels (**ASICs**) are voltage-insensitive cation channels activated by extracellular acidosis (ASIC1-3) (Waldmann *et al.*, 1997) and lipids (**ASIC3**) (Marra *et al.*, 2016). They are widely expressed throughout the peripheral and central nervous system where they have been implicated in various pathophysiological processes including pain (Deval and Lingueglia, 2015). Most subunits are expressed in TG neurons, where **ASIC1**- and **ASIC3**-containing channels can contribute to the activation of meningeal afferents (Yan *et al.*, 2011; Yan *et al.*, 2013) and the pathophysiology of migraine (Dussor, 2015). **ASIC1a** and **ASIC2a** are

expressed by second-order neurons of the TNC (Cho *et al.*, 2015), and brain **ASIC1a**-containing channels have been implicated in CSD (Holland *et al.*, 2012).

Peptide toxins from animal venoms specifically targeting different ASIC subtypes have been instrumental in revealing their roles in pain (Mazucca *et al.*, 2007; Deval *et al.*, 2008; Bohlen *et al.*, 2011; Baron *et al.*, 2013); these include mambalgins that exert potent analgesic effects against acute, inflammatory and neuropathic pain through specific inhibition of **ASIC1a**- and/or **ASIC1b**-containing channels (Diocot *et al.*, 2012; Diocot *et al.*, 2016). Using mambalgin-1 (Mamb-1) in combination with **amiloride**, a non-specific ASIC blocker, we explored the involvement of **ASIC1**-containing channels in mechanical cephalic and extra-cephalic cutaneous allodynia in the ISDN-induced model of migraine in rodents.

Methods

Animals

Experiments were performed on male Sprague Dawley rats (Janvier Labs, St Berthevin, France) weighing 250 to 400 g (mean weight: 306 ± 12 g, 6 to 9 weeks old), and on male C57BL/6J wild-type (Charles River Laboratories, L'arbresle, France) and **ASIC1a**-knockout mice (Wemmie *et al.*, 2002) of 7- to 13-weeks-old weighing 20–25 g. Animals were housed in a 12 h light–dark cycle with food and water available *ad libitum*. Animal studies are reported in compliance with the ARRIVE guidelines (Kilkenny *et al.*, 2010). Animal procedures were approved by the Institution's Local Ethical Committee and authorized by the French Ministry of Research according to the European Union regulations and the Directive 2010/63/EU (Agreements C061525 and 01550.03). Animals were killed at experimental end points by CO_2 inhalation.

Drugs and in vivo injections

Synthetic Mamb-1, showing the same pharmacological activity as the native peptide, was purchased from Synprosis/Provepep (Fuveau, France), Smartox (Saint Martin d'Hères, France), or obtained from Commissariat à l'Énergie Atomique, iBiTecS, Service d'Ingénierie Moléculaire des Protéines (Gif sur Yvette, France) (Mourier *et al.*, 2016). The biological activity of all synthetic Mamb-1 batches was validated on heterologously-expressed recombinant ASIC channels.

Mamb-1 was dissolved in vehicle solution containing NaCl 0.9% and BSA 0.05% to prevent non-specific toxin adsorption. For i.v. injections in rats, Mamb-1 ($11.3 \text{ nmol}\cdot\text{kg}^{-1}$, i.e. $200 \mu\text{L}$ of $16.5 \mu\text{M}$ for a 300 g rat), amiloride hydrochloride hydrate ($10 \text{ mg}\cdot\text{kg}^{-1}$, i.e. $200 \mu\text{L}$ of 56 mM for a 300 g rat, Sigma Aldrich, St Quentin Fallavier, France), topiramate ($30 \text{ mg}\cdot\text{kg}^{-1}$, i.e. $500 \mu\text{L}$ of $18 \text{ mg}\cdot\text{mL}^{-1}$ for a 300 g rat, Selleckchem, Munich, Germany), all dissolved in vehicle solution, or sumatriptan succinate ($10 \text{ mg}\cdot\text{kg}^{-1}$, i.e. $250 \mu\text{L}$ of an injectable $12 \text{ mg}\cdot\text{mL}^{-1}$ solution for a 300 g rat, Imject®, GlaxoSmithKline, Marly-le-Roi, France) were injected in the caudal vein of conscious rats (restrained in a cylinder) with a 30G needle. For intraplantar s.c. (i.pl.) injections, Mamb-1 ($6.7 \text{ nmol}\cdot\text{kg}^{-1}$, i.e. $50 \mu\text{L}$ of $41 \mu\text{M}$ for a 300 g rat) was injected in the left hindpaw of conscious rats with a 26G needle. For

mice, Mamb-1 (13.6 nmol·kg⁻¹, i.e. 200 µL of 1.7 µM for a 25 g mouse) dissolved in vehicle solution was i.v. injected in the caudal vein of conscious mice (restrained in a cylinder) with a 30G needle. The effects seen in our study with amiloride, sumatriptan and topiramate are consistent with the known pharmacokinetics of these drugs administered *via* the i.v. route in rodents.

Thermal and mechanical sensitivity measurements

Thermal sensitivity was assessed using the Hargreaves plantar test (Ugo Basile, Italy). Unrestrained rats were placed in individual plastic boxes on a glass floor. The withdrawal latency (s) of the rat hindpaw exposed to an infrared source (intensity of 190 ± 1 mW·cm⁻²) was measured in triplicate with at least 1 min between two stimulations, and the mean latency was calculated. A cut-off period of 20s was used to avoid potential tissue damage. Rats were trained for 2 days before the experiments. To test the effect of Mamb-1, thermal sensitivity was measured every 15 min before (basal value) and for 2 h after the Mamb-1 or vehicle injection.

The mechanical sensitivity of the face was measured using calibrated von Frey filaments (Bioseb, France). Unrestrained rats placed in individual plastic boxes on top of a wire surface were trained over 1 week; a stimulus was applied to the periorbital area, following a progressive protocol, starting with non-noxious filaments during the first 3 days of training. The face withdrawal force threshold (g) was determined by the filament evoking at least three responses over five trials, starting with lower force filaments. To test the effect of ISDN, mechanical sensitivity of the face was measured every 15 min before (basal value) and for 3 h after the i.p. injection. To test the effect of Mamb-1 and other compounds, face mechanical sensitivity was measured every 15 min before (basal value) and for 2 h after compound or vehicle injection.

The hindpaw mechanical sensitivity was evaluated with a dynamic plantar aesthesiometer (Ugo Basile). Unrestrained rats were placed in six individual plastic boxes on top of a wire surface. The rat hindpaw was subjected to a force ramped up to 30 g during 20 s, the paw withdrawal force threshold (g) was measured in triplicate, and the mean force was calculated. For 5 days, rats were habituated to repeated (every 15 min) measurements of face and hindpaw mechanical sensitivities, and basal values were determined 2 days before the experiments. To test the effect of ISDN, the hindpaw mechanical sensitivity was measured every 15 min before (basal value) and for 3 h after the i.p. injection. To test the effect of Mamb-1 and other drugs, the hindpaw mechanical sensitivity was measured every 15 min before (basal value) and for 2 h after the injection. For mice, the same procedure was used to measure the hindpaw mechanical sensitivity, except that a force ramped up to 7.5 g during 10 s was applied every 30 min and 12 mice could be tested simultaneously.

Pain and migraine rodent models

Local inflammation was induced by i.pl. injection, into a rat left hindpaw, of 100 µL of 2% carrageenan (Sigma Aldrich) with a 25G needle. Thermal and mechanical sensitivity were measured before (basal values) and 3 h after the carrageenan

injection to measure the thermal hyperalgesia and mechanical allodynia induced by inflammation (control values). Effects of drugs were followed by performing these measurements every 15 min for 2 h after their injection.

The rat model of NO-induced migraine was induced by i.p. injection of 10 mg·kg⁻¹ ISDN (Risordan®, Sanofi, Paris, France), a long-lasting NO donor, and is referred to as the ISDN-induced model in the text. The cephalic and hindpaw extra-cephalic mechanical sensitivities were measured simultaneously on the same rat. The acute mechanical allodynia induced by a single ISDN injection was followed for 3 h after injection. Chronic mechanical allodynia was induced by a single daily injection of ISDN during 4 days. Cephalic and extra-cephalic mechanical sensitivity were measured each day before the ISDN i.p. injection. Effects of drugs on chronic mechanical allodynia were tested on the fifth day and were followed every 15 min for 2 h after injection. This model has been transposed to mice using the same protocol, except that only the hindpaw extra-cephalic mechanical sensitivity was measured.

Control (or vehicle treated) and test animals were randomized within experimental sessions. Drug and peptide injections were not performed blindly in these experiments (implemented since) and data collection, analysis and statistics were performed and validated by two independent experimenters.

Data and statistical analysis

For behavioural experiments, kinetics of effects are shown, displayed as mean ± SEM as a function of time, along with cumulative effect over 2 h after injection of drugs, or over 3 h after ISDN injection, calculated as AUC (g × min for mechanical sensitivity, or s × min for thermal sensitivity) subtracted from the control value for each animal and expressed as mean ± SEM with individual data points shown. Total effect (AUC) = ∫ dYxdT, with dY the relative variation Y_{max}-Y_{control} of the measured parameter (withdrawal force or latency), and dT the time interval between two successive measurements (usually 15 min).

The power calculation was performed with an α value of 0.05 and a power of 0.8 with G*Power software, to calculate the minimum sample size per group needed depending on the expected variability of measurements (which differs between behavioural tests) and the type of statistical test to be used. For example, for the rat experiments, the minimum calculated sample size was 8 with effect sizes between 1.6 and 1.1. As most of our behavioural experiments and pharmacological treatments were not previously tested, and to anticipate the possible occurrence of non-respondent animals to pre-required treatments by carrageenan or ISDN, we set our usual minimum experimental sample size to 9. This 'n' value refers to independent values and not technical replicates (replicates were used to calculate a mean individual value). Control (or vehicle treated) animals and test animals were randomized within experimental days. Data are presented as mean values ± SEM. Data analysis and statistics were performed with Microcal Origin 6.0 and GraphPad Prism 4 softwares by two independent experimenters. The normality of data distribution was tested by KS normality test, D'Agostino and Pearson omnibus normality test and Shapiro-Wilk normality test, and parametric or non-parametric tests were

chosen for normal or non-normal data distribution respectively. Non-parametric tests were used when the number of animals per experimental group was less than 10, because the results of normality tests were not totally reliable in these conditions. The statistical difference between two different experimental groups was analysed by the parametric Student's unpaired *t*-test or by the non-parametric Mann–Whitney test. The statistical difference between more than two different experimental groups was assessed by the parametric one-way ANOVA followed by a Tukey's *post-hoc* test, or by the non-parametric Kruskal–Wallis test followed by a Dunn's *post-hoc* test. For data within the same experimental group, a parametric Student's paired *t*-test or a non-parametric Wilcoxon matched pairs test was used. The level of probability $P < 0.05$ denotes a statistically significant differences between groups, and *post-hoc* tests were only run when $P < 0.05$.

Nomenclature of targets and ligands

Key protein targets and ligands in this article are hyperlinked to corresponding entries in <http://www.guidetopharmacology.org>, the common portal for data from the IUPHAR/BPS Guide to PHARMACOLOGY (Harding *et al.*, 2018), and are permanently archived in the Concise Guide to PHARMACOLOGY 2017/18 (Alexander *et al.*, 2017a,b).

Results

Anti-allodynic effects of *i.v.* mambalgin-1 against inflammatory pain in rats

Mambalgins exert analgesic effects in mice upon different routes of administration (*i.pl.*, *i.v.*, *i.t.*, *i.c.v.*) and against different types of pain, including inflammatory pain (Diochot *et al.*, 2012; Diochot *et al.*, 2016). However, their effects in rats were never tested. Before using the ISDN-induced model of migraine for simultaneous measurements of cephalic and extra-cephalic mechanical sensitivity, we first determined the effect of Mamb-1 on inflammatory pain in rats by testing a single dose extrapolated from the maximal effective concentration previously determined in mice from an *in vivo* dose–response curve (Diochot *et al.*, 2016). Three hours after *i.pl.* injection of 2% carrageenan in the hindpaw, mechanical allodynia was observed, with a decrease in withdrawal threshold force from 18.4 ± 0.5 g down to 9.2 ± 0.2 g (Figure 1A), as well as thermal hyperalgesia, with a decrease in withdrawal latency from 9.0 ± 0.3 s down to 4.3 ± 0.2 s (Figure 1B). An *i.v.* injection of Mamb-1 ($11.3 \text{ nmol}\cdot\text{kg}^{-1}$) induced a complete and sustained reversal of the inflammatory-induced mechanical allodynia (Figure 1A, 19.1 ± 0.8 g after 45 min), as well as a

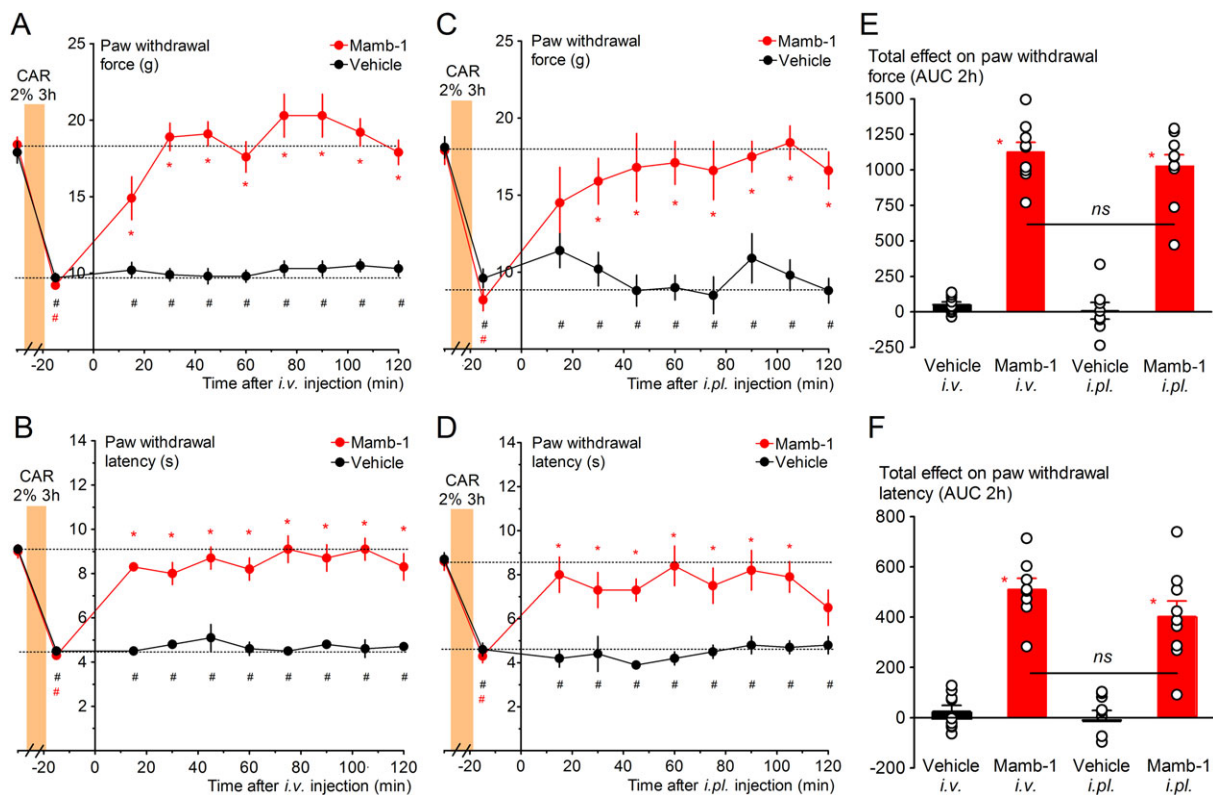


Figure 1

Reversal of inflammation-induced paw mechanical allodynia and thermal hyperalgesia by *i.v.* and local intraplantar (*i.pl.*) injections of mambalgin-1 in rats. (A, C) Full reversal by *i.v.* (A) and by *i.pl.* (C) Mamb-1 (11.3 and $6.7 \text{ nmol}\cdot\text{kg}^{-1}$ respectively) of paw inflammatory mechanical allodynia (carrageenan 2%, 3 h). (B, D) Full reversal by *i.v.* (B) and *i.pl.* (D) Mamb-1 of paw inflammatory thermal hyperalgesia (carrageenan 2%, 3 h). (A–D) Results are shown as mean \pm SEM, $n = 9$. $*P < 0.05$ compared to vehicle with Mann–Whitney non-parametric test, $\#P < 0.05$ compared to control non-inflamed basal value with Wilcoxon matched paired test. (E, F) Total effect of *i.v.* and of *i.pl.* Mamb-1 on paw mechanical withdrawal force (E) and on heat paw withdrawal latency (F) calculated as the AUC during the 2 h after the injection. Individual data points and mean \pm SEM are shown; $n = 9$. $*P < 0.05$ compared to vehicle with Mann–Whitney non-parametric test.

complete reversal of the inflammatory-induced thermal hyperalgesia (Figure 1B, 8.7 ± 0.5 s, after 45 min). Local i.pl. injection of Mamb-1 in the rat-inflamed hindpaw ($6.7 \text{ nmol}\cdot\text{kg}^{-1}$) also resulted in a complete and sustained reversal of the inflammatory-induced mechanical allodynia (Figure 1C) and thermal hyperalgesia (Figure 1D). The kinetics and total effects of Mamb-1 were comparable between i.v. and i.pl. injections (Figure 1C–F). However, i.pl. and i.v. injections of Mamb-1 had no effect on hindpaw mechanical threshold in naive rats (Supporting Information Figure S1).

These data indicate that i.v. or i.pl. Mamb-1 exert anti-allodynic effects on inflammatory pain in rats, comparable to the effects we already described in mice that were mainly peripheral and caused by the inhibition of ASIC1b-containing channels (Diochot *et al.*, 2016).

Effect of i.v. mambalgin-1 and amiloride on acute cutaneous mechanical allodynia in the ISDN-induced model of migraine

The ISDN-induced chronic migraine model was developed recently in rats (Flores Ramos *et al.*, 2017; Dallel *et al.*, 2018), related to the chronic NTG-induced model first developed in mice (Pradhan *et al.*, 2014). One i.p. injection of ISDN ($10 \text{ mg}\cdot\text{kg}^{-1}$) induces mechanical allodynia mimicking what is occurring during a migraine attack, with a decrease in cephalic and extra-cephalic mechanical sensitivity. The facial and hindpaw withdrawal force thresholds reached their minimal values after 1.5 h (3.3 ± 0.4 from a basal control value of 7.5 ± 0.3 g; and 12.2 ± 0.4 from a basal control value of 17.8 ± 0.2 g respectively) that were maintained for at least 3 h, whereas i.p. injections of saline were without effect (Supporting Information Figure S2A,B, black symbols, left panels). Twenty four hours later, an allodynia was still present, and one ISDN injection per day for 4 days resulted in the progressive development of a chronic basal mechanical allodynia (2.4 ± 0.3 g on the face, and 10.1 ± 0.3 g on the paw; Supporting Information Figure S2C,D), which was correlated with a progressive decrease in the ISDN-induced cephalic and extra-cephalic total effect on acute cutaneous allodynia, the last injection inducing no more significant effect (Supporting Information Figure S2A,B, right panels). The chronic basal mechanical allodynia persisted several days after the last ISDN injection, and a nearly total reversal was observed 15 days after the end of ISDN treatment (Supporting Information Figure S2C,D).

The effect of i.v. Mamb-1 on the acute mechanical allodynia induced by the first ISDN injection was tested. When Mamb-1 was injected after the full development of acute allodynia (i.e. 105 min after ISDN i.p. injection), it induced a full reversal of facial mechanical allodynia (Figure 2A), the withdrawal force increasing from the allodynic value of 3.3 ± 0.5 g up to 7.6 ± 0.4 g 1 h after the i.v. injection, which is not significantly different from the baseline (8.0 ± 0.3 g). On the same animals, Mamb-1 only induced a partial reversal of the hindpaw mechanical allodynia, the withdrawal force increasing from the allodynic value of 11.2 ± 0.5 g up to 14.0 ± 1.3 g 1 h after the i.v. injection (Figure 2B). These effects were sustained for at least 2 h. The anti-allodynic effect of i.v. Mamb-1, which significantly reduced the total effects of the first injection of ISDN on cutaneous allodynia, induced a 1 day shift in the development of chronic allodynia induced by subsequent daily i.p.

injections of ISDN in both cephalic and extra-cephalic regions, without any change in the maximal basal allodynia measured on the last day (Figure 2C,D). This supports, as suggested in humans, a causality link between occurrence of attack-like mechanical allodynia and the development of chronic allodynia.

The effect of i.v. Mamb-1 on ISDN-induced acute mechanical allodynia was compared with that of amiloride, a well-known non-selective inhibitor of ASICs, and also with that of the acute migraine therapy sumatriptan, a **5-HT_{1B}** and **5-HT_{1D}** receptor agonist. Amiloride or sumatriptan succinate, both i.v. injected in the same conditions as Mamb-1, also exerted an anti-allodynic effect. Amiloride induced a full reversal of face mechanical allodynia (Figure 3A) and a partial but significant reversal of hindpaw allodynia (Figure 3B), similar to the sustained Mamb-1 effects. As expected from its therapeutic effect, and as previously described in mice models of migraine (Bates *et al.*, 2010; Pradhan *et al.*, 2014), sumatriptan also showed sustained anti-allodynic properties, with a partial reversal of both facial (Figure 3A) and hindpaw (Figure 3B) allodynia.

All together, these data show that systemic i.v. Mamb-1 and amiloride effectively reverse the ISDN-induced cephalic, and to a lesser extent extra-cephalic, mechanical acute cutaneous allodynia, with an even higher potency than sumatriptan.

Effects of i.v. mambalgin-1 and amiloride on the maximal chronic cutaneous mechanical allodynia in the ISDN-induced model of migraine

When Mamb-1 was injected 1 day after the last ISDN injection (i.e. on the fifth day), it fully reversed the maximal chronic facial mechanical allodynia (Figure 4A), increasing the facial withdrawal force from 3.0 ± 0.4 g up to 9.6 ± 2.1 g after 1 h, to a value similar to baseline (8.6 ± 0.9 g). Mamb-1 also partially reversed the maximal chronic hindpaw mechanical allodynia (Figure 4B), increasing the paw withdrawal force from 9.8 ± 0.2 g up to 15.0 ± 1.1 g after 1 h to a value significantly different from vehicle as well as from baseline (18.0 ± 0.2 g). Amiloride also showed similar anti-allodynic effects (Figure 4A,B). Both compounds were as potent as topiramate, a clinically used preventive drug against migraine, whereas sumatriptan, used in acute migraine therapy, was ineffective (Figure 4C–F), as previously described (Pradhan *et al.*, 2014). Local i.pl. injection of Mamb-1, which was able to reverse inflammatory-induced mechanical paw allodynia (Figure 1C), was without effect on ISDN-induced chronic paw mechanical allodynia (Supporting Information Figure S3) showing that the local inhibition of ASICs in sensory neurons of the paw was not involved in the anti-allodynic effect of Mamb-1 on the paw ISDN-induced allodynia, contrary to the effects on inflammatory pain. Furthermore, the absence of effect of i.pl. injection of Mamb-1 on chronic facial ISDN-induced allodynia (Supporting Information Figure S3), contrary to what is observed after i.v. injection, confirmed that the effect of the peptide upon i.pl. injection remains local without important systemic diffusion towards blood.

These data show that systemic i.v. Mamb-1 and amiloride efficiently reverse the maximal chronic cephalic and extra-cephalic cutaneous mechanical allodynia with a potency similar to topiramate.

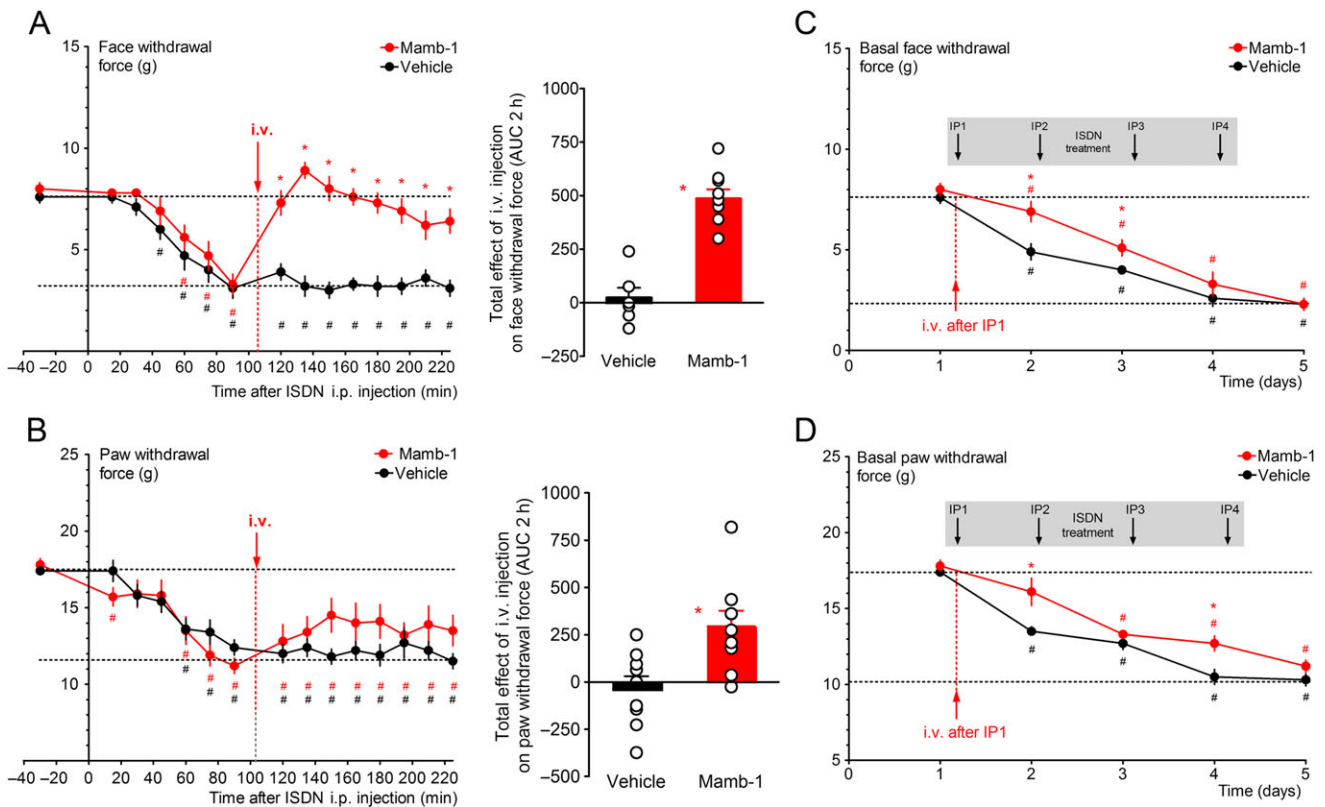


Figure 2

Reversal of ISDN-induced cephalic and extra-cephalic acute mechanical allodynia by an i.v. injection of mambalgin-1. (A, B – left panels) Kinetics of the anti-allodynic effect on face (A) and paw (B) mechanical withdrawal thresholds (g) of an i.v. injection of Mamb-1 ($11.3 \text{ nmol}\cdot\text{kg}^{-1}$) 105 min after the i.p. injection of ISDN in rats. Mean \pm SEM, $n = 9$: * $P < 0.05$ compared to vehicle with Mann–Whitney non-parametric test; # $P < 0.05$ compared to control value before ISDN injection with Wilcoxon matched paired test. (A, B – right panels) Total effect of i.v. Mamb-1 (or vehicle) on face (A) and paw (B) withdrawal force calculated as the AUC during the 2 h after the i.v. injection. Individual data points and mean \pm SEM, $n = 9$, * $P < 0.05$ compared to vehicle with Mann–Whitney non-parametric test. (C, D) One i.v. injection of Mamb-1 ($11.3 \text{ nmol}\cdot\text{kg}^{-1}$) after the first ISDN injection, as shown in A and B, induces a delay in the subsequent generation of ISDN-evoked chronic allodynia induced by three more daily ISDN injections. Basal face (C) and paw (D) mechanical withdrawal force (g) measured before each daily ISDN injection and the day after the last ISDN injection (day 5). Mean \pm SEM, $n = 9$: * $P < 0.05$ compared to vehicle with Mann–Whitney non-parametric test; # $P < 0.05$ compared to control before the first ISDN injection with Wilcoxon matched paired test.

Preventive effect of i.v. mambalgin-1 treatment on the development of chronic cutaneous mechanical allodynia in the ISDN-induced migraine model

Mamb-1 was able to reverse the maximal chronic cutaneous allodynia induced by 4 days of ISDN injections. We tested next the effects of one daily i.v. injection of Mamb-1 for 4 days, between ISDN-induced attacks and their consequences on the development of chronic allodynia.

In good agreement with the data showing no effect of i.v. injection of Mamb-1 on basal paw mechanical threshold in naive rats (Supporting Information Figure S1), the i.v. injection of Mamb-1 30 min before the first i.p. injection of ISDN did not change the basal face and paw mechanical sensitivities (Figure 5A,B, black symbols). The acute effect of ISDN with the maximal allodynia reaching $5.3 \pm 0.5 \text{ g}$ from the basal level of $8.2 \pm 0.2 \text{ g}$ on the face, and $13.7 \pm 0.3 \text{ g}$ from a basal level of $18.5 \pm 0.2 \text{ g}$ on the paw after 2h (Figure 5A,B, black symbols), was not significantly different from that seen in vehicle injected rats (Figure 5C,D, black symbols). A basal

allodynia appeared the day after (i.e. on day 2; Figure 5E,F) that was reversed by Mamb-1, i.v. injected 30 min before the second ISDN injection (Figure 5A,B, red symbols), whereas vehicle was without effect (Figure 5C,D, red symbols). On day 3, the basal cutaneous allodynia was significantly less pronounced in Mamb-1-treated compared to vehicle-treated rats, reaching $5.1 \pm 0.4 \text{ g}$ on the face and $14.7 \pm 0.3 \text{ g}$ on the paw, and $2.9 \pm 0.4 \text{ g}$ on the face and $13.4 \pm 0.2 \text{ g}$ on the paw, respectively (Figure 5E,F). Repeated i.v. injections of Mamb-1 on days 3 and 4 finally led to a significant reduction in the maximal chronic allodynia on day 5, that is, 24 h after the last ISDN injection, reaching $4.7 \pm 0.3 \text{ g}$ on face and $13.8 \pm 0.5 \text{ g}$ on paw, compared to $1.9 \pm 0.3 \text{ g}$ and $11.5 \pm 0.4 \text{ g}$, respectively, on vehicle-treated rats (Figure 5E,F). Consequently, an ISDN-induced acute increase in allodynia was still observed in Mamb-1-treated rats on the fourth day (Figure 5A,B, blue symbols), but not in vehicle-treated rats already close to the maximal allodynic level (Figure 5C,D, blue symbols).

Our results show that a daily “inter-attack” i.v. injection of Mamb-1 was able to significantly reduce the chronic

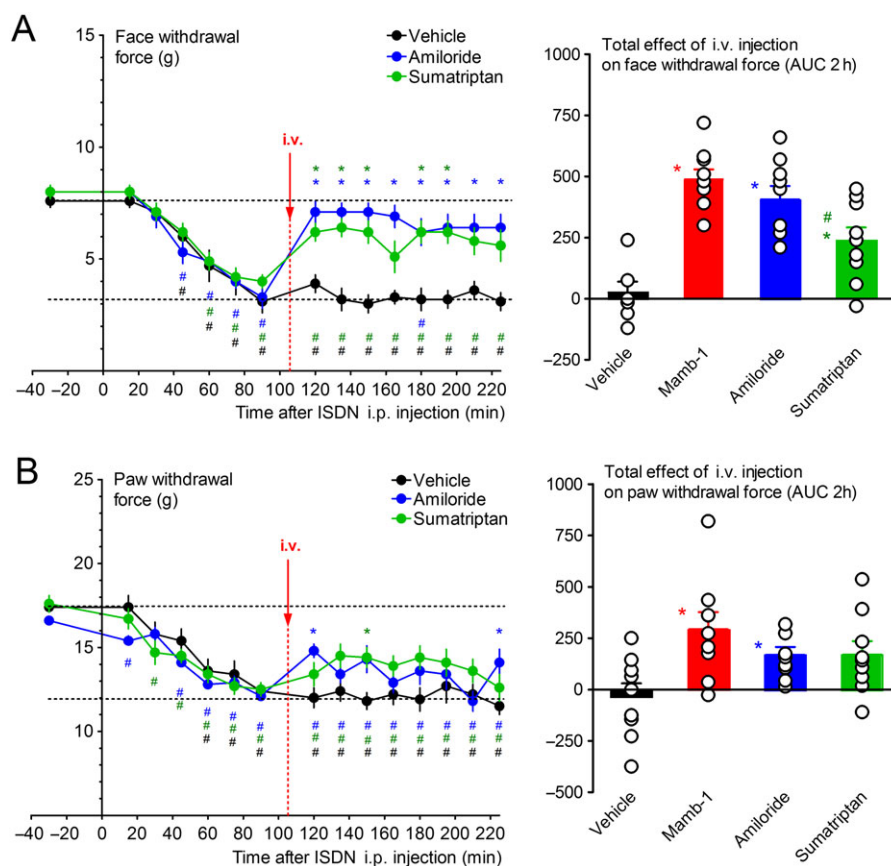


Figure 3

Comparison of the anti-allodynic effects of mambalgin-1, amiloride and sumatriptan on ISDN-induced cephalic and extra-cephalic acute mechanical allodynia. (A, B, left panels) Kinetics of the analgesic effects on face (A) and paw (B) mechanical withdrawal force (g), of amiloride ($10 \text{ mg}\cdot\text{kg}^{-1}$) and sumatriptan succinate (Imiject[®], $10 \text{ mg}\cdot\text{kg}^{-1}$) i.v. injected 105 min after the injection of ISDN measured on the same rats. Mean \pm SEM, $n = 9$. * $P < 0.05$ with non-parametric Kruskal–Wallis and Dunn's *post hoc* tests compared to vehicle; # $P < 0.05$ with Wilcoxon matched paired test compared to control value before ISDN injection. For clarity, only vehicle (same data as in Figure 2A,B) but not Mamb-1 is shown. (A, B, right panels) Total effect of vehicle, Mamb-1 (same data as in Figure 2A,B), amiloride and sumatriptan on face (A) and paw (B) withdrawal force, calculated as the AUC, during the 2 h after injection. Individual data points and mean \pm SEM, $n = 9$: * $P < 0.05$ with Mann–Whitney non-parametric test compared to vehicle; # $P < 0.05$ with Mann–Whitney non-parametric test compared to Mamb-1.

allodynia that develops upon injection of ISDN for several days, especially on the facial region, without affecting normal cutaneous sensitivity or the ability of ISDN to induce an acute allodynic effect. The absence of a preventive effect of Mamb-1 i.v. injected 30 min before the first ISDN injection could be due to the limited half-life of Mamb-1 in blood circulation regarding the 30 to 90 min needed after ISDN injection (i.e. 60 to 120 min after Mamb-1 injection) for allodynia to develop (Supporting Information Figure S2).

The anti-allodynic effect of i.v. mambalgin-1 in the ISDN-induced chronic migraine model is still present in ASIC1a knockout mice

Since Mamb-1 inhibits ASIC1-containing channels (i.e. comprising either ASIC1a and/or ASIC1b subunits), the contribution of ASIC1a to its anti-allodynic effects in the ISDN-induced chronic migraine model was tested on hindpaw mechanical sensitivity in ASIC1a-knockout (KO) mice. In wild-type mice, the first i.p. injection of ISDN induced an acute paw allodynia, with the withdrawal force decreasing from $4.1 \pm 0.1 \text{ g}$ down to $3.0 \pm$

0.1 g 2 h after the ISDN injection (Figure 6A, black symbols). Allodynia was not fully reversed the next day, and one ISDN injection per day for 4 days resulted, like in rats, in the progressive development of a chronic mechanical allodynia correlated with a progressive decrease in the daily total effect of ISDN, leading to the absence of effect of the fourth ISDN injection (Figure 6A, blue symbols). On day 5 (i.e. 24 h after the last ISDN injection), the maximal chronic allodynia reaches $2.7 \pm 0.1 \text{ g}$ from a control (day 1) value of $4.1 \pm 0.1 \text{ g}$ and was reversed towards control mechanical sensitivity by an i.v. injection of Mamb-1 (Figure 6B). Interestingly, the reversal of chronic paw allodynia was complete in mice, whereas only partial in rats. The same experiments have been done in ASIC1a-KO mice and showed no difference with wild-type animals either in the ISDN-induced acute allodynia (at day 1 and at day 4) (Figure 6C) or in the development of chronic allodynia (reaching $2.6 \pm 0.1 \text{ g}$ from a control (day 1) value of $4.1 \pm 0.1 \text{ g}$, not significantly different from wild-type mice with Mann–Whitney non-parametric test) and in the anti-allodynic effects of i.v. Mamb-1 on the maximal chronic allodynia (Figure 6D).

These data show that ASIC1a is not needed for the anti-allodynic effects of Mamb-1 or for the establishment of the

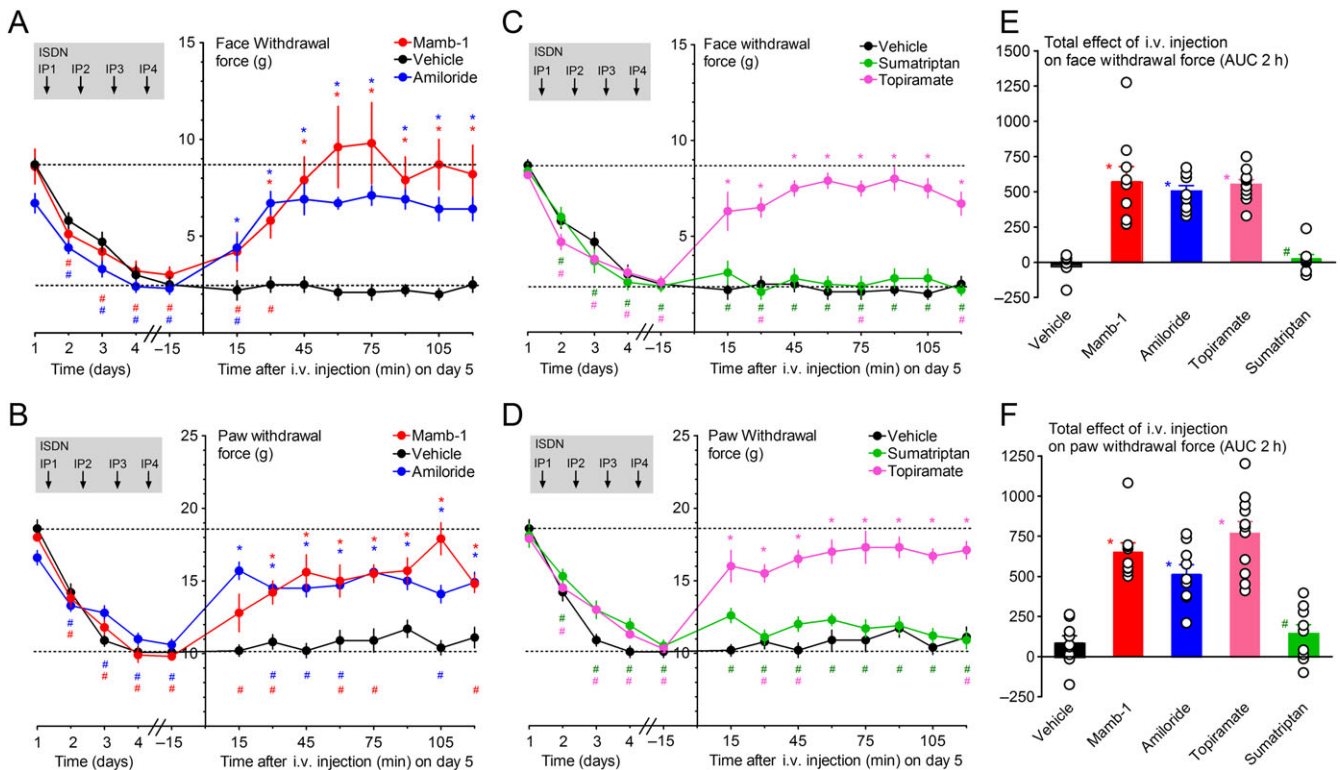


Figure 4

Reversal of ISDN-induced maximal cephalic and extra-cephalic chronic mechanical allodynia by an i.v. injection of mambalgin-1. (A–D) Kinetics of the anti-allodynic effect of Mamb-1 ($11.3 \text{ nmol}\cdot\text{kg}^{-1}$), amiloride ($10 \text{ mg}\cdot\text{kg}^{-1}$), sumatriptan succinate (Imiject, $10 \text{ mg}\cdot\text{kg}^{-1}$) and topiramate ($30 \text{ mg}\cdot\text{kg}^{-1}$), i.v. injected 1 day after the last ISDN injection (i.e. on day 5) on face (A, C) and paw (B, D) mechanical withdrawal force (g) in rats. The basal mechanical withdrawal force (g) was measured before each daily ISDN injection (left side of the y axis), showing the chronification process of cutaneous allodynia day after day. For clarity, kinetics were split into two graphs, sharing the same data for vehicle. Mean \pm SEM, $n = 9$ except with topiramate ($n = 11$). * $P < 0.05$ with Mann–Whitney non-parametric test compared to vehicle; # $P < 0.05$ with Wilcoxon matched paired test compared to control value before the first ISDN injection (day 1), not shown, but all significant for vehicle. (E, F) Total effect on face (E) and paw (F) withdrawal force calculated as the AUC during the 2 h after the i.v. injection for each rat. Individual data points and mean \pm SEM $n = 9$: * $P < 0.05$ with Mann–Whitney non-parametric test compared to vehicle; # $P < 0.05$ with Mann–Whitney non-parametric test compared to Mamb-1.

ISDN-induced migraine model in mice. They also indicate that ISDN has a similar effect in mice as in rats after repetitive daily injections with the establishment of a maximal chronic basal allodynia, which is consistent with that previously described with nitroglycerin as the NO-donor (Pradhan *et al.*, 2014).

Discussion

In this study, we demonstrated the anti-allodynic effects of i.v. ASIC1 inhibitors in a rodent model of migraine induced by daily i.p. injection of ISDN, a long-lasting NO-donor. Mambalgin-1 and amiloride reverse cephalic and extra-cephalic cutaneous allodynia when i.v. injected during the attack-like acute effect of one ISDN injection, with an effect similar to that of sumatriptan, and caused a delay in the establishment of chronic allodynia induced by subsequent ISDN injections. ASIC1 inhibitors are also able to reverse the maximal cephalic and extra-cephalic chronic allodynia when i.v. injected after the four injections of ISDN, with an effect similar to that of topiramate. A daily “inter-attack” i.v. injection of Mamb-1 is able to significantly reduce

maximal cutaneous allodynia, thus exerting a preventive effect on the establishment of chronic allodynia.

Involvement of peripheral ASIC1-containing channels in migraine-induced cutaneous allodynia and in its chronification

The contribution of ASIC1 channels in acute and chronic cutaneous allodynia in the ISDN-induced migraine model is strongly supported by the similar anti-allodynic effects of amiloride, a well described non-selective inhibitor of ASICs, and Mamb-1, a specific inhibitor of ASIC1-containing channels (Diochot *et al.*, 2012). Mamb-1, in contrast to amiloride, does not block the **epithelial sodium channel** involved in blood pressure regulation (Supporting Information Figure S4), making it unlikely that these compounds have a significant indirect vascular contribution in the ISDN-induced migraine model. In rodents, Mamb-1 only inhibits ASIC1a- and ASIC1b-containing channels, with ASIC1a expressed in both central and sensory neurons (small diameter neurons), and ASIC1b exclusively expressed in sensory neurons (small to large diameter neurons) (Chen *et al.*,

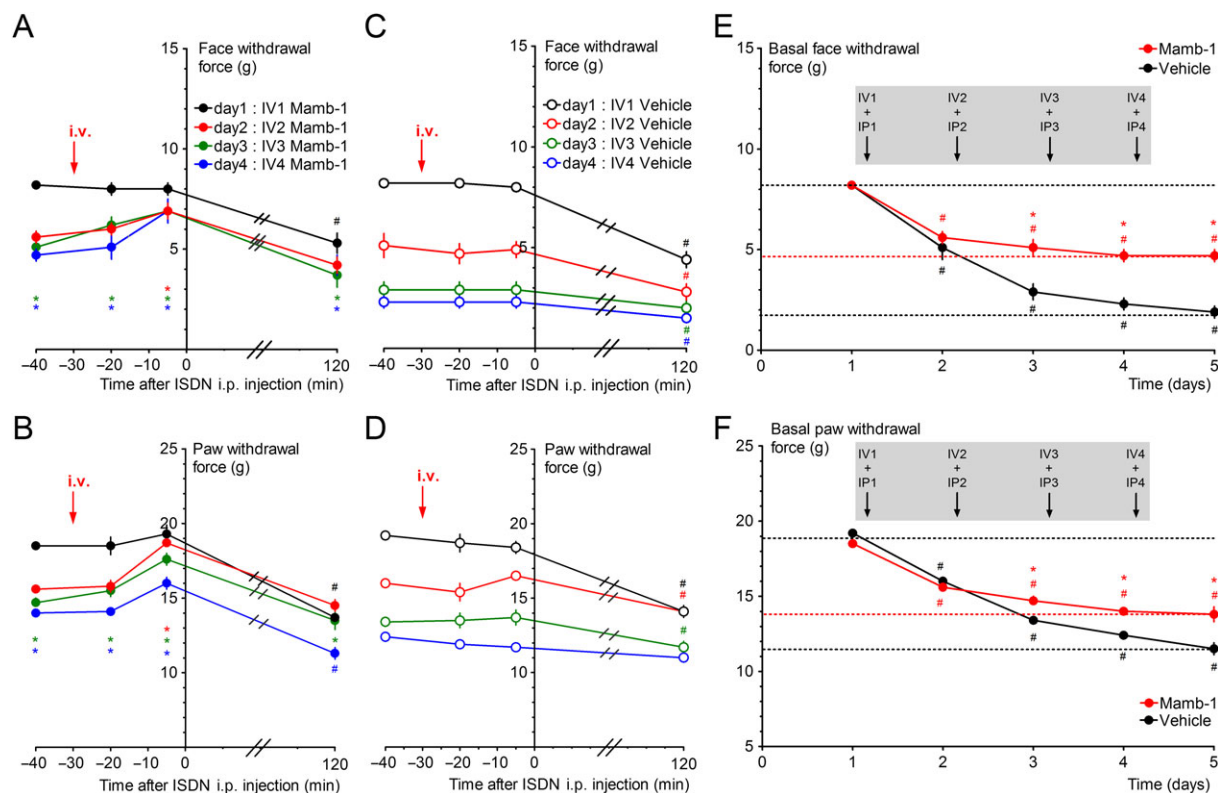


Figure 5

Preventive effect of i.v. Mamb-1 treatment on chronification of cephalic and extra-cephalic mechanical allodynia. (A–D) Kinetics of the effects of a daily i.v. injection of Mamb-1 ($11.3 \text{ nmol}\cdot\text{kg}^{-1}$, A, B) or vehicle (C, D) 30 min before each daily ISDN injection ($10 \text{ mg}\cdot\text{kg}^{-1}$) on face (A, C) and paw (B, D) mechanical withdrawal threshold (g). Mean \pm SEM, $n = 9$: * $P < 0.05$ with Mann–Whitney non-parametric test compared to vehicle; # $P < 0.05$ with Wilcoxon matched paired test compared to baseline value before any injection. (E, F) Effects of a daily i.v. injection of Mamb-1 or vehicle (same conditions as in A–D) on the basal face (E) and paw (F) mechanical withdrawal force threshold (g) measured on the same rats before each daily i.v. injection (values at time -40 on graphs A–D) and after the last, fourth, ISDN injection (day 5). Mean \pm SEM, $n = 9$. * $P < 0.05$ with Mann–Whitney non-parametric test compared to vehicle; # $P < 0.05$ with Wilcoxon matched paired test compared to control before injection.

1998). We have previously shown that the central effects of Mamb-1 are totally lost in ASIC1a-KO mice (Diochot *et al.*, 2012; Diochot *et al.*, 2016). ASIC1a is not necessary for the anti-allodynic effect of i.v. Mamb-1 in the ISDN-induced migraine model. This precludes a major contribution of central ASIC1a-containing channels and supports a peripheral effect involving ASIC1b specifically expressed in sensory neurons, although a direct demonstration would need genetic ablation of ASIC1b in TG neurons. However, native ASICs are composed of three identical or different subunits, and the contribution of peripheral ASIC1a subunits in wild-type animals cannot be ruled out, for instance, within heteromeric channels made up of ASIC1a and ASIC1b. Our results are also in good agreement with our previous data in mice showing a major role for peripheral ASIC1b-containing channels in the analgesic effect of i.v. mambalgin-1 on inflammatory pain (Diochot *et al.*, 2016).

Peripheral ASIC1-containing channels in TG sensory fibres could be therefore be involved in the pathophysiology of migraine, possibly correlated with meningeal extracellular acidification as one of the initiating events. Our results support the involvement of ASICs that can be activated by NO-induced extracellular acidification (through mast cells

degranulation) and further stimulated by inflammatory mediators and associated transduction pathways. ASIC1- and ASIC3-containing channels were proposed as important pain detectors in sensory neurons of the orofacial area (Fu *et al.*, 2016) notably in the dura mater (Yan *et al.*, 2011; Yan *et al.*, 2013; Burgos-Vega *et al.*, 2015). About 80% of rat dural afferents trigger action potentials at pH 6.0, 50% at pH 7.0 and 30% at pH 7.1. As a consequence, an acidic pH 6.0 solution applied on dura mater generates sustained cephalic and extra-cephalic allodynia, which is maximal after 2 h and inhibited by amiloride but not TRPV1 antagonists, supporting the involvement of ASICs activation in migraine-related behaviour *in vivo* (Yan *et al.*, 2011; Yan *et al.*, 2013). ASIC3-containing channels have been proposed to be involved in these effects (Yan *et al.*, 2013), as well as in the potentiating effects of inflammatory factors, and our data now also support the involvement of ASIC1-containing channels (presumably ASIC1b) since Mamb-1 does not inhibit ASIC3-containing channels (Diochot *et al.*, 2012). Interestingly, Mamb-1 was shown to modify the pH-dependent activation and inactivation curves of ASIC1a channels (Diochot *et al.*, 2012; Salinas *et al.*, 2014) with a higher inhibitory potency in conditions of mild acidosis, which are

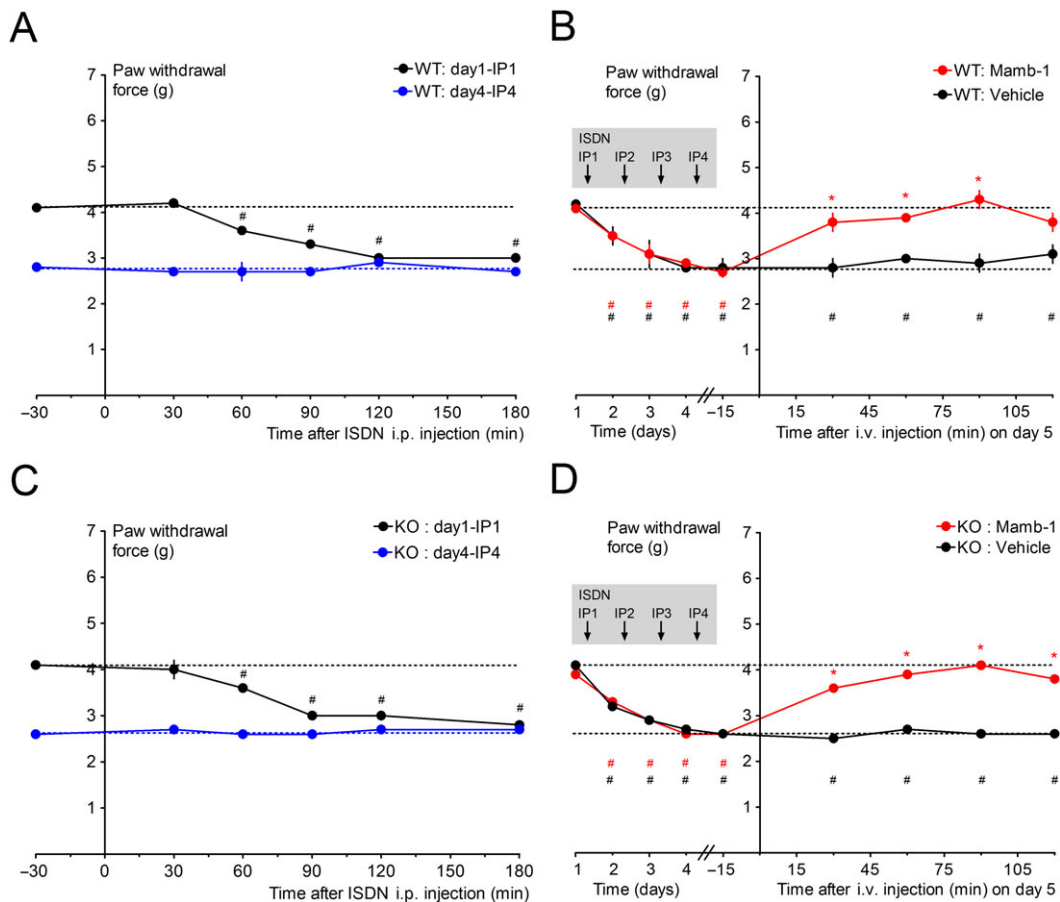


Figure 6

Reversal of ISDN-induced maximal extra-cephalic chronic mechanical allodynia by an i.v. injection of mambalgin-1 in wild-type and ASIC1a knockout (KO) mice. (A, C) Kinetics of the effects of the first ISDN injection on day 1 and of the fourth ISDN injection on day 4 on hindpaw mechanical withdrawal threshold (g) of wild-type (A, $n = 20$) and ASIC1a-KO (C, $n = 17$) mice. Mean \pm SEM, $^{\#}P < 0.05$ with Wilcoxon matched paired test compared to control value before the ISDN injection, all non-significant for day 4 data. (B, D) Kinetics of the anti-allodynic effect of Mamb-1 ($13.6 \text{ nmol}\cdot\text{kg}^{-1}$) and vehicle i.v. injected 1 day after the last ISDN injection (i.e. on day 5) on paw mechanical withdrawal force (g) of wild-type (B, $n = 10$) and ASIC1a-KO (D, $n = 8-9$) mice. The basal mechanical withdrawal force (g) was measured before each daily ISDN injection (left side of the Y axis, which includes the values at -30 min for day 1 and 4 in A and C), showing the chronification process of cutaneous allodynia day after day. Mean \pm SEM, $n = 8-10$. $^*P < 0.05$ with Mann-Whitney non-parametric test compared to vehicle; $^{\#}P < 0.05$ with Wilcoxon matched paired test compared to control value before the first ISDN injection (day 1). Groups of mice used in A and C were then divided in half to be injected with either vehicle or Mamb-1, as shown in B and D.

thought to happen around sensory nerves terminals in pathological conditions such as inflammation or migraine triggering. In addition to ASIC3-containing channels, which are expressed in 80% of pH-sensitive dural fibres (Yan *et al.*, 2013), the ASIC1a, ASIC1b and ASIC2 subunits were also present in TG neurons (Manteniots *et al.*, 2013; Cho *et al.*, 2015; Flegel *et al.*, 2015; Fu *et al.*, 2016), and data obtained with ASIC1a-KO mice support the involvement of ASIC1-like currents in TG ganglion in orofacial inflammatory pain (Fu *et al.*, 2016). Transcriptome analyses recently showed higher expression of ASIC1 in TG versus lumbar DRG neurons (Lopes *et al.*, 2017). Another interesting point concerns the NO potentiation of ASICs in heterologous systems as well as in rat sensory neurons (Cadiou *et al.*, 2007), with transient effects on ASIC1a, ASIC2a and ASIC3 currents, but an irreversible effect on rat ASIC1b current that could also contribute to the role of ASIC1b in the ISDN-induced model.

Inhibition of peripheral ASIC1-containing channels in TG afferents by systemic Mamb-1 and amiloride could thus participate in the analgesic effects seen in the ISDN-induced rat migraine model. Local i.pl. injection of Mamb-1 in the paw was not able to reverse ISDN-induced chronic paw mechanical allodynia, whereas it fully reversed the inflammatory-induced one. The systemic extra-cephalic, anti-allodynic effect of i.v. Mamb-1 would thus not be due to local inhibition of peripheral sensory ASIC1-containing channels in the paw but would rather be a consequence of the reversal of cephalic ISDN-induced allodynia through inhibition of ASIC1-containing channels in TG sensory fibres. Peripheral sensitization of the TG sensory neurons leads to secondary central sensitization of the second order neurons of the TNC and upper cervical spinal cord (C1-C2), thus causing subsequent cephalic allodynia, whereas extra-cephalic allodynia would reflect the further extension of central

sensitization to upper central pain relays (like thalamus), particularly during the settlement of a chronic state (Boyer *et al.*, 2014). Highly diffusible NO is also able to directly exert central effects, with modulation of medullary dorsal horn neurons (Flores Ramos *et al.*, 2017), TNC neurons and VPM thalamus neurons (Goadsby *et al.*, 2017), thus amplifying cutaneous pain sensitization. The anti-allodynic and anti-chronification effects of ASIC1 inhibitors are weaker on extra-cephalic than on cephalic allodynia in our experiments in rats. Similar incomplete effects were reported for amiloride in another rat migraine model with a direct dural acidic stimulation (Yan *et al.*, 2013) and in a mice NTG-induced model of chronic migraine (Tipton *et al.*, 2016). The complete reversibility of cephalic allodynia by ASIC1 inhibitors that we observed would suggest that sensitization of the TNC and the upper cervical dorsal horn could depend directly on the activity of TG sensory neurons expressing ASIC1-containing channels, whereas extra-cephalic allodynia would be partially independent of them, involving central mechanisms independent of TG fibres activation (Bernstein and Burstein, 2012) or ASIC-independent effects of NO on paw sensory fibres (Ferrari *et al.*, 2016).

Systemic ASIC1 blockers against migraine

Treatment of migraine, and particularly chronic migraine, remains challenging, and numerous therapeutic drugs are non-specific, sometimes inefficient, with side effects and contraindications (Serrano *et al.*, 2015; Schytz *et al.*, 2017). Cutaneous allodynia in chronic migraine is associated with inadequate outcomes for any anti-migraine medication (Lipton *et al.*, 2017). Furthermore, a significant proportion of chronic migraine cases are due to anti-migraine medication abuse or misuse (Bigal and Lipton, 2009; Lipton *et al.*, 2015), highlighting the need for new medications, including new prophylactic approaches to prevent the chronification process.

We showed that i.v. amiloride and mambalgin-1 both exert long-lasting anti-allodynic effects against acute and chronic cutaneous allodynia in the ISDN-induced migraine model, not only in extra-cephalic regions, as usually assessed, but also in cephalic ones, and that i.v. mambalgin-1 is able to exert a prophylactic effect on the development of chronic allodynia, without affecting normal cutaneous sensitivity. This supports systemic (among which orally administered) ASIC1 inhibitors as new potential therapeutic leads against migraine and headaches, and this is in good agreement with data showing that a preventive daily therapy with i.p. amiloride in mice partially reduces acute NTG-induced as well as chronic basal mechanical paw hypersensitivity (Tipton *et al.*, 2016). A pilot open clinical study has also shown that systemic treatment with amiloride reduced aura and headache symptoms in four of seven patients with intractable aura (Holland *et al.*, 2012). The drawback of amiloride, which is used in humans as a diuretic and antihypertensive, is its poor specificity, and our data suggest that more specific ASIC1 blockers like mambalgin-1 could also be used (i) to relieve migraine attack, with benefits on subsequent chronification, (ii) to relieve established chronic allodynia and (iii) as a preventive treatment against chronification.

Acknowledgements

We thank R. Dallel for initial help with the ISDN-induced model in rats and discussion, D. Servent for providing synthetic mambalgin-1, E. Deval, P. Inquimbert, J. Noël, M. Salinas, M. Chafai, S. Marra and T. Besson for helpful discussions, M. Lazdunski for his support, V. Friend for expert technical assistance, and V. Berthieux for secretarial assistance. This work was supported by the Centre National de la Recherche Scientifique, the Institut National de la Santé et de la Recherche Médicale, the Fondation pour la Recherche Médicale (DEQ20110421309) and the Agence Nationale de la Recherche (ANR-13-BSV4-0009, ANR-17-CE18-0019 and ANR-11-LABX-0015-01).

Author contributions

C.V., E.P., M.L.M., E.L. and A.B. designed the research. C.V., E.P., S.D., M.D. and A.B. performed the research, and C.V., E.P., S.D., M.L.M., E.L. and A.B. wrote the paper.

Conflict of interest

The authors declare no conflicts of interest.

Declaration of transparency and scientific rigour

This Declaration acknowledges that this paper adheres to the principles for transparent reporting and scientific rigour of preclinical research recommended by funding agencies, publishers and other organisations engaged with supporting research.

References

- Alexander SPH, Christopoulos A, Davenport AP, Kelly E, Marrion NV, Peters JA *et al.* (2017a). The Concise Guide to PHARMACOLOGY 2017/18: G protein-coupled receptors. *Br J Pharmacol* 174: S17–S129.
- Alexander SP, Peters JA, Kelly E, Marrion NV, Faccenda E, Harding SD *et al.* (2017b). The Concise Guide to PHARMACOLOGY 2017/18: ligand-gated ion channels. *Br J Pharmacol* 174: S130–S159.
- Ashina M, Hansen JM, Olesen J (2013). Pearls and pitfalls in human pharmacological models of migraine: 30 years' experience. *Cephalalgia* 33: 540–553.
- Baron A, Diochot S, Salinas M, Deval E, Noel J, Lingueglia E (2013). Venom toxins in the exploration of molecular, physiological and pathophysiological functions of acid-sensing ion channels. *Toxicon* 75: 187–204.
- Bates EA, Nikai T, Brennan KC, Fu YH, Charles AC, Basbaum AI *et al.* (2010). Sumatriptan alleviates nitroglycerin-induced mechanical and thermal allodynia in mice. *Cephalalgia* 30: 170–178.
- Bernstein C, Burstein R (2012). Sensitization of the trigeminovascular pathway: perspective and implications to migraine pathophysiology. *J Clin Neurol* 8: 89–99.

- Bigal ME, Lipton RB (2009). Overuse of acute migraine medications and migraine chronification. *Curr Pain Headache Rep* 13: 301–307.
- Bigal ME, Serrano D, Buse D, Scher A, Stewart WF, Lipton RB (2008). Acute migraine medications and evolution from episodic to chronic migraine: a longitudinal population-based study. *Headache* 48: 1157–1168.
- Bohlen CJ, Chesler AT, Sharif-Naeini R, Medzihradsky KF, Zhou S, King D *et al.* (2011). A heteromeric Texas coral snake toxin targets acid-sensing ion channels to produce pain. *Nature* 479: 410–414.
- Boyer N, Dallel R, Artola A, Monconduit L (2014). General trigeminospinal central sensitization and impaired descending pain inhibitory controls contribute to migraine progression. *Pain* 155: 1196–1205.
- Burgos-Vega C, Moy J, Dussor G (2015). Meningeal afferent signaling and the pathophysiology of migraine. *Prog Mol Biol Transl Sci* 131: 537–564.
- Burstein R, Jakubowski M, Garcia-Nicas E, Kainz V, Bajwa Z, Hargreaves R *et al.* (2010). Thalamic sensitization transforms localized pain into widespread allodynia. *Ann Neurol* 68: 81–91.
- Cadiou H, Studer M, Jones NG, Smith ES, Ballard A, McMahon SB *et al.* (2007). Modulation of acid-sensing ion channel activity by nitric oxide. *J Neurosci* 27: 13251–13260.
- Chen CC, England S, Akopian AN, Wood JN (1998). A sensory neuron-specific, proton-gated ion channel. *Proc Natl Acad Sci U S A* 95: 10240–10245.
- Cho JH, Choi IS, Nakamura M, Lee SH, Lee MG, Jang IS (2015). Proton-induced currents in substantia gelatinosa neurons of the rat trigeminal subnucleus caudalis. *Eur J Pharmacol* 762: 18–25.
- Dallel R, Descheemaeker A, Luccarini P (2018). Recurrent administration of the nitric oxide donor, isosorbide dinitrate, induces a persistent cephalic cutaneous hypersensitivity: a model for migraine progression. *Cephalalgia* 38: 776–785.
- Deval E, Lingueglia E (2015). Acid-sensing ion channels and nociception in the peripheral and central nervous systems. *Neuropharmacology* 94: 49–57.
- Deval E, Noel J, Lay N, Alloui A, Diochot S, Friend V *et al.* (2008). ASIC3, a sensor of acidic and primary inflammatory pain. *EMBO J* 27: 3047–3055.
- Diochot S, Alloui A, Rodrigues P, Dauvois M, Friend V, Aissouni Y *et al.* (2016). Analgesic effects of mambalgin peptide inhibitors of acid-sensing ion channels in inflammatory and neuropathic pain. *Pain* 157: 552–559.
- Diochot S, Baron A, Salinas M, Douguet D, Scarzello S, Dabert-Gay AS *et al.* (2012). Black mamba venom peptides target acid-sensing ion channels to abolish pain. *Nature* 490: 552–555.
- Dussor G (2015). ASICs as therapeutic targets for migraine. *Neuropharmacology* 94: 64–71.
- Edelmayer RM, Vanderah TW, Majuta L, Zhang ET, Fioravanti B, De Felice M *et al.* (2009). Medullary pain facilitating neurons mediate allodynia in headache-related pain. *Ann Neurol* 65: 184–193.
- Farkas S, Bolcskei K, Markovics A, Varga A, Kis-Varga A, Kormos V *et al.* (2016). Utility of different outcome measures for the nitroglycerin model of migraine in mice. *J Pharmacol Toxicol Methods* 77: 33–44.
- Ferrari LF, Levine JD, Green PG (2016). Mechanisms mediating nitroglycerin-induced delayed-onset hyperalgesia in the rat. *Neuroscience* 317: 121–129.
- Flegel C, Schobel N, Altmüller J, Becker C, Tannapfel A, Hatt H *et al.* (2015). RNA-Seq analysis of human trigeminal and dorsal root ganglia with a focus on chemoreceptors. *PLoS One* 10: e0128951.
- Flores Ramos JM, Devoize L, Descheemaeker A, Molat JL, Luccarini P, Dallel R (2017). The nitric oxide donor, isosorbide dinitrate, induces a cephalic cutaneous hypersensitivity, associated with sensitization of the medullary dorsal horn. *Neuroscience* 344: 157–166.
- Fu H, Fang P, Zhou HY, Zhou J, Yu XW, Ni M *et al.* (2016). Acid-sensing ion channels in trigeminal ganglion neurons innervating the orofacial region contribute to orofacial inflammatory pain. *Clin Exp Pharmacol Physiol* 43: 193–202.
- Goadsby PJ, Holland PR, Martins-Oliveira M, Hoffmann J, Schankin C, Akerman S (2017). Pathophysiology of migraine: a disorder of sensory processing. *Physiol Rev* 97: 553–622.
- Hansen EK, Olesen J (2017). Towards a pragmatic human migraine model for drug testing: 2. Isosorbide-5-mononitrate in healthy individuals. *Cephalalgia* 37: 11–19.
- Harding SD, Sharman JL, Faccenda E, Southan C, Pawson AJ, Ireland S *et al.* (2018). The IUPHAR/BPS guide to PHARMACOLOGY in 2018: updates and expansion to encompass the new guide to IMMUNOPHARMACOLOGY. *Nucl Acids Res* 46: D1091–D1106.
- Harris HM, Carpenter JM, Black JR, Smitherman TA, Sufka KJ (2017). The effects of repeated nitroglycerin administrations in rats; modeling migraine-related endpoints and chronification. *J Neurosci Methods* 284: 63–70.
- Holland PR, Akerman S, Andreou AP, Karsan N, Wemmie JA, Goadsby PJ (2012). Acid-sensing ion channel 1: a novel therapeutic target for migraine with aura. *Ann Neurol* 72: 559–563.
- Iversen HK, Nielsen TH, Garre K, Tfelt-Hansen P, Olesen J (1992). Dose-dependent headache response and dilatation of limb and extracranial arteries after three doses of 5-isosorbide-mononitrate. *Eur J Clin Pharmacol* 42: 31–35.
- Jansen-Olesen I, Tfelt-Hansen P, Olesen J (2013). Animal migraine models for drug development: status and future perspectives. *CNS Drugs* 27: 1049–1068.
- Karatas H, Erdener SE, Gursoy-Ozdemir Y, Lule S, Eren-Kocak E, Sen ZD *et al.* (2013). Spreading depression triggers headache by activating neuronal Panx1 channels. *Science* 339: 1092–1095.
- Kilkenny C, Browne W, Cuthill IC, Emerson M, Altman DG (2010). Animal research: reporting *in vivo* experiments: the ARRIVE guidelines. *Br J Pharmacol* 160: 1577–1579.
- Levy D (2009). Migraine pain, meningeal inflammation, and mast cells. *Curr Pain Headache Rep* 13: 237–240.
- Lipton RB, Bigal ME, Ashina S, Burstein R, Silberstein S, Reed ML *et al.* (2008). Cutaneous allodynia in the migraine population. *Ann Neurol* 63: 148–158.
- Lipton RB, Fanning KM, Serrano D, Reed ML, Cady R, Buse DC (2015). Ineffective acute treatment of episodic migraine is associated with new-onset chronic migraine. *Neurology* 84: 688–695.
- Lipton RB, Munjal S, Buse DC, Bennett A, Fanning KM, Burstein R *et al.* (2017). Allodynia is associated with initial and sustained response to acute migraine treatment: results from the American migraine prevalence and prevention study. *Headache* 57: 1026–1040.
- Lopes DM, Denk F, McMahon SB (2017). The molecular fingerprint of dorsal root and trigeminal ganglion neurons. *Front Mol Neurosci* 10: 1–11.

- Louter MA, Bosker JE, van Oosterhout WP, van Zwet EW, Zitman FG, Ferrari MD *et al.* (2013). Cutaneous allodynia as a predictor of migraine chronification. *Brain* 136: 3489–3496.
- Manteniots S, Lehmann R, Flegel C, Vogel F, Hofreuter A, Schreiner BS *et al.* (2013). Comprehensive RNA-Seq expression analysis of sensory ganglia with a focus on ion channels and GPCRs in Trigeminal ganglia. *PLoS One* 8: e79523.
- Marra S, Ferru-Clement R, Breuil V, Delaunay A, Christin M, Friend V *et al.* (2016). Non-acidic activation of pain-related acid-sensing ion channel 3 by lipids. *EMBO J* 35: 414–428.
- Mazucca M, Heurteaux C, Alloui A, Diochot S, Baron A, Voilley N *et al.* (2007). A tarantula peptide against pain via ASIC1a channels and opioid mechanisms. *Nat Neurosci* 10: 943–945.
- Mourier G, Salinas M, Kessler P, Stura EA, Leblanc M, Tepshi L *et al.* (2016). Mambalgin-1 pain-relieving peptide, stepwise solid-phase synthesis, crystal structure, and functional domain for acid-sensing ion channel 1a inhibition. *J Biol Chem* 291: 2616–2629.
- Nahman-Averbuch H, Shefi T, Schneider VJ 2nd, Li D, Ding L, King CD *et al.* (2018). Quantitative sensory testing in patients with migraine: a systematic review and meta-analysis. *Pain* 159: 1202–1223.
- Olesen J, Ashina M (2015). Can nitric oxide induce migraine in normal individuals? *Cephalalgia* 35: 1125–1129.
- Pradhan AA, Smith ML, McGuire B, Tarash I, Evans CJ, Charles A (2014). Characterization of a novel model of chronic migraine. *Pain* 155: 269–274.
- Rozniecki JJ, Dimitriadou V, Lambracht-Hall M, Pang X, Theoharides TC (1999). Morphological and functional demonstration of rat dura mater mast cell-neuron interactions *in vitro* and *in vivo*. *Brain Res* 849: 1–15.
- Salinas M, Besson T, Delettre Q, Diochot S, Boulakirba S, Douguet D *et al.* (2014). Binding site and inhibitory mechanism of the mambalgin-2 pain-relieving peptide on acid-sensing ion channel 1a. *J Biol Chem* 289: 13363–13373.
- Scher AI, Buse DC, Fanning KM, Kelly AM, Franznick DA, Adams AM *et al.* (2017). Comorbid pain and migraine chronicity: the chronic migraine epidemiology and outcomes study. *Neurology* 89: 461–468.
- Schytz HW, Hargreaves R, Ashina M (2017). Challenges in developing drugs for primary headaches. *Prog Neurobiol* 152: 70–88.
- Serrano D, Buse DC, Manack Adams A, Reed ML, Lipton RB (2015). Acute treatment optimization in episodic and chronic migraine: results of the American migraine prevalence and prevention (AMPP) study. *Headache* 55: 502–518.
- Thomsen LL, Brennum J, Iversen HK, Olesen J (1996). Effect of a nitric oxide donor (glyceryl trinitrate) on nociceptive thresholds in man. *Cephalalgia* 16: 169–174.
- Tipton AF, Tarash I, McGuire B, Charles A, Pradhan AA (2016). The effects of acute and preventive migraine therapies in a mouse model of chronic migraine. *Cephalalgia* 36: 1048–1056.
- Vos T, Allen C, Arora M, Barber RM, Bhutta ZA, Brown A *et al.* (2016). Global, regional, and national incidence, prevalence, and years lived with disability for 310 diseases and injuries, 1990–2015: a systematic analysis for the Global Burden of Disease Study 2015. GBD 2015 disease and injury incidence and prevalence collaborators. *Lancet* 388: 1545–1602.
- Waldmann R, Champigny G, Bassilana F, Heurteaux C, Lazdunski M (1997). A proton-gated cation channel involved in acid-sensing. *Nature* 386: 173–177.
- Wemmie JA, Chen J, Askwith CC, Hruska-Hageman AM, Price MP, Nolan BC *et al.* (2002). The acid-activated ion channel ASIC contributes to synaptic plasticity, learning, and memory. *Neuron* 34: 463–477.
- Yan J, Edelmayer RM, Wei X, De Felice M, Porreca F, Dussor G (2011). Dural afferents express acid-sensing ion channels: a role for decreased meningeal pH in migraine headache. *Pain* 152: 106–113.
- Yan J, Wei X, Bischoff C, Edelmayer RM, Dussor G (2013). pH-evoked dural afferent signaling is mediated by ASIC3 and is sensitized by mast cell mediators. *Headache* 53: 1250–1261.

Supporting Information

Additional supporting information may be found online in the Supporting Information section at the end of the article.

<https://doi.org/10.1111/bph.14462>

Figure S1 Absence of effect of intravenous and local intraplantar injections of mambalgin-1 on paw mechanical sensitivity of naive rats.

Figure S2 Migraine-like, ISDN-induced cephalic and extra-cephalic acute and chronic mechanical allodynia.

Figure S3 Absence of effect of intraplantar injection of mambalgin-1 on ISDN-induced cephalic and extra-cephalic chronic mechanical allodynia.

Figure S4 Mambalgin-1 does not inhibit the epithelial sodium channel.